Published in final edited form as:

Cell Metab. 2017 April 04; 25(4): 868–882.e5. doi:10.1016/j.cmet.2017.02.004.

Insulin signaling regulates the FoxM1/PLK1/CENP-A pathway to promote adaptive pancreatic β-cell proliferation

Jun Shirakawa[1], **Megan Fernandez**[1], **Tomozumi Takatani**[1], **Abdelfattah El Ouaamari**[1], **Prapaporn Jungtrakoon**[2], **Erin R. Okawa**[1], **Wei Zhang**[1], **Peng Yi**[1], **Alessandro Doria**[2], and **Rohit N. Kulkarni**[1]

[1]Islet Cell and Regenerative Biology, Joslin Diabetes Center, Department of Medicine, Brigham and Women's Hospital, Harvard Stem Cell Institute, Harvard Medical School, Boston, MA 02215, USA

[2]Section on Genetics and Epidemiology, Joslin Diabetes Center and Harvard Medical School, Boston, MA 02215, USA

Summary

Investigation of cell cycle kinetics in mammalian pancreatic β-cells has mostly focused on transition from the quiescent (G0) to G1 phase. Here we report that centromere protein A (CENP-A), which is required for chromosome segregation during the M-phase, is necessary for adaptive β-cell proliferation. Receptor-mediated insulin signaling promotes DNA-binding activity of FoxM1 to regulate expression of CENP-A and polo-like kinase-1 (PLK1) by modulating cyclin dependent kinase-1/2. CENP-A deposition at the centromere is augmented by PLK1 to promote mitosis while knocking down CENP-A limits β-cell proliferation and survival. CENP-A deficiency in β-cells leads to impaired adaptive proliferation in response to pregnancy, acute and chronic insulin resistance, and aging in mice. Insulin-stimulated CENP-A/PLK1 protein expression is blunted in islets from patients with type 2 diabetes. These data implicate the insulin-FoxM1/PLK1/CENP-A pathway-regulated mitotic cell cycle progression as an essential component in the β-cell adaptation to delay and/or prevent progression to diabetes.

Graphical abstract

*Correspondence to: rohit.kulkarni@joslin.harvard.edu.
Lead Contact: Rohit N. Kulkarni (rohit.kulkarni@joslin.harvard.edu)

Author Contributions

J.S. conceived the idea, designed and performed experiments, analyzed the data, and wrote the manuscript. M.F. conducted contributed to generation, maintenance of knockout mice. T.T. contributed to cell culture experiments in vitro. A.E.O. contributed to human islet samples preparations. E.O. contributed to animal studies and discussion. P.J. and A.D. provided data on the PLK1 variant. W.Z. and P.Y. provided data on S961 injection study. R.N.K. conceived the idea, contributed to experimental design, analyzed the data, wrote/edited/reviewed the manuscript, and contributed to discussions. R.N.K. is the guarantor of this work. All authors read and approved the manuscript.

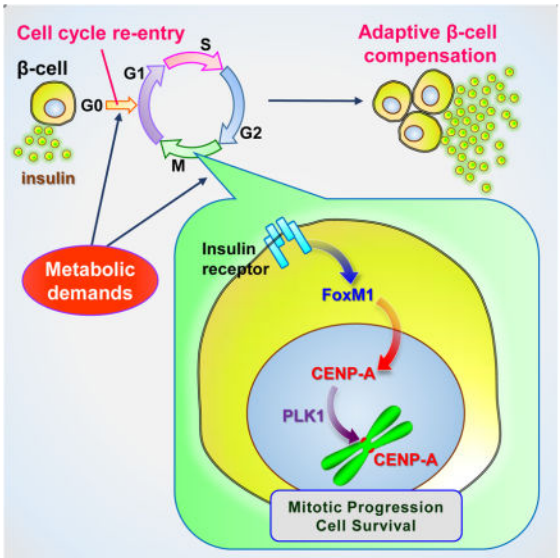

Keywords

β-cell proliferation; cell cycle; CENP-A; PLK1; FoxM1; type 2 diabetes; insulin signaling

Introduction

β-cell dysfunction in type 2 diabetes (T2DM) patients occurs secondary to inappropriate insulin secretory response to glucose and a reduction in β-cell volume. A decreased β-cell mass is a consistent feature in T2DM (Meier et al., 2008; Rahier et al., 2008) and provides a strong rationale to explore the cellular mechanism(s) that regulate β-cell mass especially in the context of an adaptive response to insulin resistance. In addition to acute glucose stimulation, which promotes β-cell proliferation and survival by modulating proteins in the growth factor (insulin/insulin-like growth factor-1) signaling pathway (Assmann et al., 2009; Demozay et al., 2011; Shirakawa et al., 2013), recent studies have implicated several other proteins to enhance human β-cell replication some of which act by modulating proteins in the insulin/IGF-1 signaling pathway (Dhawan et al., 2016; Dirice et al., 2016; El Ouaamari et al., 2016; Hayes et al., 2016; Kondegowda et al., 2015; Shirakawa and Kulkarni, 2016; Wang et al., 2015). In pancreatic islets obtained from T2DM donors, the mRNA expression of several proteins in the insulin/IGF-1 signaling cascade are reduced compared with islets from non-diabetes controls (Folli et al., 2011; Gunton et al., 2005; Muller et al., 2006). These data are consistent with studies in rodents manifesting varying degrees of reduced β-cell mass and/or diabetes following conditional disruption of one or more proteins in the growth factor signaling pathway (Bernal-Mizrachi et al., 2004; Kubota et al., 2004; Kulkarni et al., 1999a; Okada et al., 2007; Terauchi et al., 2007; Withers et al., 1999). Other studies indicate that some proteins (e.g. IGF-1 receptor) are dispensable for the maintenance of β-cell mass (Kulkarni et al., 2002; Xuan et al., 2002). However, it is unclear whether downregulation of one or more growth factor-mediated signals directly impacts proteins that regulate cell cycle progression in the compensatory response of the β-cells. The islet β-cell

is among the most differentiated mammalian cell types, and adult β-cells are largely quiescent (in the G0 phase of the cell cycle). Growth factors including insulin are known to promote G0/G1 transition and regulate the G1/S check point in the cell cycle in human β-cells (Fiaschi-Taesch et al., 2013). However, the identity of signaling proteins that precisely regulate the G2/M checkpoint, a critical phase that determines whether a cell progresses to mitosis and becomes mature or chooses death, are not fully understood (DiPaola, 2002). These observations prompted us to focus on a previously unexplored link between growth factor signaling pathways and the distal cell cycle checkpoint (e.g. G2/M) in β-cells.

In this study, we report reduced expression of two M-phase related molecules, centromere protein-A (CENP-A) and polo-like kinase-1 (PLK1) in β-cell-specific insulin receptor knockout (βIRKO) β-cells. CENP-A, a centromere-specific histone H3 variant, is required for recruitment and assembly of kinetochore proteins, mitotic progression and chromosome segregation in mammalian cells (Foltz et al., 2006). PLK1 plays important roles during the mitotic phase, especially in the regulation of entry and exit of mitosis (Bruinsma et al., 2012), and is reportedly essential for the deposition of CENP-A at the centromere (McKinley and Cheeseman, 2014). Our data provides evidence for insulin receptor-mediated regulation of the FoxM1/PLK1/CENP-A pathway in β-cells that is critical for cell proliferation and survival during the adaptive compensatory response.

Results

Insulin regulates CENP-A and PLK1 gene expression in pancreatic β-cells

We began by assessing cell cycle abundance by analyzing DNA content using propidium iodide (PI) staining in control and βIRKO mouse β-cell lines (Okada et al., 2007) using flow cytometry. Compared to controls, βIRKO β-cells showed a significant increase in the ratio of G0/G1-phase cells while the proportions of S-phase and G2/M-phase cells were significantly decreased (Figure S1A, **upper panels**). Separating the M-phase cells from G2-phase cells using an M-phase-specific marker, serine 28-phophorylated histone H3, revealed that the M-phase cells in the G2/M-phase fraction were significantly increased supporting the presence of an M-phase arrest in βIRKO cells (Figure S1A, **lower panels**). Our previous studies on gene expression microarray analysis of freshly isolated islets and β-cell lines derived from βIRKO mice revealed several novel targets of insulin-receptor signaling including M-phase-related genes that were significantly down-regulated (data not shown). In this study, we focused on two proteins that were downregulated in βIRKOs, namely CENP-A (<10% compared to control) and PLK1 (~60% compared to control), since they are functionally related to chromosome segregation during the M phase (Kang et al., 2006; Regnier et al., 2005).

We first confirmed that the expression of CENP-A and PLK1 was significantly decreased in primary β-cells obtained from βIRKO mice compared to control (IR-floxed) mice using immunohistochemistry (Figure 1A) and immunoblotting (Figure S1B). Similarly, the βIRKO β-cell line exhibited significantly lower CENP-A and PLK1 expression compared to the control β-cell line (Figure 1B, S1C, S1D). The expression of CENP-A and PLK1 also tended to be decreased in β-cells lacking the insulin receptor substrate-2 (IRS2KO), but not in IRS1KO β-cells (Figure 1B, S1C, S1D). An M-phase related gene NEK1, but not CENP-

B or MELK, showed decreased expression in βIRKO and increased expression in IRS1KO β-cells (Figure S1D). While the expression of CENP-A peaked ~4h (G2 phase) after release from cell cycle synchronization at the G1/S boundary using a double thymidine block, PLK1 expression gradually increased until 12h to 24h (M to G1-phase; pHH3: M-phase marker) (Figure 1C). These changes in CENP-A and PLK1 abundance during cell cycle progression are consistent with previous reports (Park et al., 2015; Shelby et al., 1997). In βIRKO cells, CENP-A protein was significantly reduced and its peak expression was delayed to 6–12h; and PLK1 was virtually undetectable throughout the cell cycle (Figure 1C). Re-expression of human wild-type insulin receptor in βIRKO cells restored the expression of both CENP-A and PLK1 (Figure S1E). Furthermore, expression of a low insulin binding S323L insulin receptor mutant in βIRKO β-cells (Roach et al., 1994) showed blunted restoration of CENP-A and PLK1 protein compared to the levels observed in βIRKO cells re-expressing the wild type insulin receptor (Figure 1D) indicating insulin binding to its receptor enhances CENP-A and PLK1 expression. The transcription factor FoxM1 is thought to activate CENP-A and PLK-1 expression and to play a role in the G2/M-phase of the cell cycle (Golson et al., 2015; Wang et al., 2005). However, we did not observe significant differences in the expression of FoxM1 between control and βIRKO in either primary islets or β-cell lines (Figure 1C, S1B, S1C). Stimulation with exogenous insulin significantly increased expression of CENP-A and PLK1 protein in islets isolated from control mice (Figure 1E, 1F, S1F) and in the control β-cell line (Figure S1G). As expected insulin failed to impact the expression of CENP-A in βIRKO β-cells while treatment with IGF-1 induced CENP-A expression in both control and βIRKO β-cells (Figure S1H). Interestingly, glucose stimulation upregulated CENP-A and PLK1 expression in control but not in βIRKO β-cells (Figure S1I). The glucose effects in control β-cells was virtually completely abrogated by diazoxide, which inhibits insulin secretion by opening K^+-ATP channels (Figure S1J). These results indicate the effect of glucose on CENP-A and PLK1 expression is dependent on the insulin receptor, and is consistent with previous reports (Assmann et al., 2009; Mezza et al., 2016).

Insulin-stimulated FoxM1 binding to CENP-A and PLK1-associated DNA in the nucleus

Next we focused on localization and DNA binding capacity of FoxM1 in β-cells. FoxM1 was mostly localized to the nucleus in β-cells in both control and βIRKO mice (Figure 2A, S2A). In both control and βIRKO β-cell lines, FoxM1 was predominantly detected in the nuclear fraction before and after stimulation with insulin (Figure S2B). The MAPK/ERK kinase (MEK)1/2 inhibitor (U0126), but not the PI3-kinase inhibitor (LY294002), promoted nuclear export of FoxM1 as shown by immunocytochemistry or immunoblotting (Figure 2B, 2C). We confirmed that extracellular signal-regulated kinase (ERK) phosphorylation was not attenuated but rather enhanced in βIRKO β-cells in the basal state (Figure S2C). Unlike mouse β-cells, FoxM1 was mainly localized to the cytosol in β-cells of cultured human islets after starvation (Figure 2D). Insulin stimulation facilitated nuclear localization of FoxM1, which was restrained by MEK1/2 inhibitor, in human β-cells (Figure 2D, S2D). The transcriptional activity of FoxM1 is regulated by Chk2 and Cdk1/2 in the nucleus (Major et al., 2004; Tan et al., 2007). Expression of Cdk1 and Cdk2 was decreased in βIRKO cells, while the expression of Chk2 was not changed, compared to control β-cells (Figure 2E). IR and IGF1R dual inhibitor (OSI-906), PI3-kinase inhibitor (LY294002), and Akt inhibitor

(MK-2206) each independently attenuated insulin-induced CENP-A and PLK1 expression, as well as Cdk1 and Cdk2 protein, in control β-cells (Figure 2F). Next, examination of FoxM1 binding to CENP-A and PLK1 associated genomic DNA by ChIP analysis in β-cell lines revealed that FoxM1 was recruited to CENP-A and PLK1 genomic regions in control β-cells, while the binding was significantly reduced in the presence of the FoxM1 inhibitor, thiostrepton (Hegde et al., 2011), or in βIRKO cells (Figure 2G). As a control, lysine 14-acetylated histone H3 binding to β-actin and GAPDH promoters did not change significantly in those cells (Figure S2E). The PI3-kinase inhibitor also prevented the association of FoxM1 with CENP-A and PLK-1 associated DNA (Figure S2F, S2G). Thus, FoxM1 appears to be regulated predominantly at the level of its activation rather than transcription in β-cells.

Next, we investigated whether the insulin receptor-mediated signal also regulates the M-phase proteins in non-islet tissues. Interestingly, exogenous insulin treatment of primary hepatocytes did not significantly alter expression of CENP-A or PLK1; however, the expression of PEPCK, a positive control, was significantly reduced (Figure S2H). Conversely, we did not detect significant changes in expression of CENP-A or PLK1 in the liver (Figure S2I), white adipose tissue (Figure S2J), or brown adipose tissue (Figure S2K) obtained from mice with a conditional knockout of the insulin receptor (LIRKO, FIRKO, or Myf5IRKO mice respectively) (Bluher et al., 2002; Lynes et al., 2015; Michael et al., 2000). However, in each of these tissues the absence of functional insulin receptors was confirmed by tissue-specific changes in target genes – i.e. enhanced expression of PEPCK (LIRKO) (Figure S2I), reduced expression of sterol regulatory element-binding protein 1 (SREBP-1) (FIRKO) (Figure S2J) and enhanced expression of adipose triglyceride lipase (ATGL) (Myf5IRKO) (Figure S2K).

Insulin-induced CENP-A expression in human islets is impaired in type 2 diabetes

We next examined human islets obtained from patients with type 2 diabetes that are known to express significantly low levels of proteins in the insulin signaling pathway (Folli et al., 2011; Gunton et al., 2005). RT-PCR and qPCR analysis revealed significantly low levels of CENP-A, a trend to decreased expression of PLK1 and no significant differences in FoxM1 expression in T2DM donors compared to non-diabetes (non-DM) donors (Figure 3A, 3B, S3A). In a previous report, CENP-A expression in adult human β-cells was detectable at the mRNA level (Lee et al., 2010). Consistently, although we also detected CENP-A expression in β-cells from all 16 adult non-DM or T2DM donors, the number of CENP-A expressing β-cells was significantly attenuated in the islets from T2DM donors, despite a lack of significant changes in the ratio of CENP-A-positive non-β-cells (Figure 3C, 3D, S3B). Similar to the data in mouse samples, the expression of CENP-A and PLK1 was increased by exogenous insulin treatment of islets from non-diabetes donors (Figure 3E **upper panels**). However, in the islets from T2DM donors, the response was variable but significantly diminished consistent with reduced Akt phosphorylation upon stimulation with insulin (Figure 3E **lower panels**). The expression of FoxM1 protein was not altered between non-DM and T2DM donors in the presence or absence of insulin stimulation (Figure 3E). These observations are consistent with the notion that reduced CENP-A expression is associated with lower β-cell mass when IRS-2 or PI3K protein expression are attenuated in islets from patients with type 2 diabetes (Folli et al., 2011; Gunton et al., 2005). A potential

link to human diabetes was the identification of a missense variant of the PLK1 gene (c.A1216T, p.I406F, rs565735478) in one of 52 Joslin families with autosomal dominant diabetes that underwent whole-exome sequencing (a description of this study is provided in (Prudente et al., 2015)). This variant, having an allele frequency of 0.1% among Europeans in the 1000 Genome database, is conserved among species (GREP score=5.2, Figure S3C) and is predicted to be “disease causing” by MutationTester (with 0.99 probability) as well as other prediction softwares. All three diabetic members of the family carried this variant, which was instead absent in all four non-diabetic members (Figure S3D; for individual characteristics of family, see Table S1).

β-cell-specific CENP-A knockout (βCenpaKO) mice demonstrate reduced β-cell proliferation

To investigate the role of CENP-A in β-cells *in vivo*, we created an inducible β-cell-specific CENP-A knock-out (βCenpaKO) mouse by crossing MIP-Cre/ERT mice (Wicksteed et al., 2010) with CENP-A-floxed mice, and injecting with tamoxifen at 7-weeks of age to recombine exons 2 to 5 of the Cenpa gene (Figure S4A). We detected 80% nuclear Cre+ β-cells (Figure S4B) and βCenpaKO mice exhibited genomic recombination of Cenpa alleles and consequent diminished expression of CENP-A only in islets, and not in the hypothalamus, liver, or spleen (Figure 4A, S4C, S4D). Glucose-stimulated insulin secretion from isolated islets of 11 week-old βCenpaKO was comparable with floxed islets (Figure S4E). βCenpaKO mice showed normal body weight gain, random-fed blood glucose levels, and insulin sensitivity on chow diet (Figure S4F, S4G). While 8 or 16 week-old βCenpaKO mice had normal glucose tolerance, the knockouts developed glucose intolerance, impaired insulin secretion, decreased phospho-histone H3 (pHH3)+ mitotic and BrdU+ proliferating β-cells, and β-cell mass by 24 weeks of age (Figure 4B, 4C, 4D, 4E, S4H). MIP-Cre/ERT mice showed no significant changes in blood glucose levels, body weight, glucose tolerance, β-cell mass, or BrdU+ proliferating β-cells compared with CENP-A-floxed mice at 24 weeks of age (Figure S4I, S4J, S4K). Body weight, blood glucose levels, or circulating insulin levels at gestational day 15.5 were not changed in female βCenpaKO mice (Figure S4L, S4M). However, β-cell mass, mitosis, and proliferation during pregnancy were all attenuated in βCenpaKO mice (Figure 4F, 4G, 4H).

Next, we fed mice with high-fat diets for 16 weeks to create a diet-induced obesity (DIO) model. The body weight gain and insulin sensitivity were similar in DIO βCenpaKO mice in both genders (Figure S5A, S5B). But after 6 weeks, both male and female DIO βCenpaKO mice manifested hyperglycemia compared with floxed mice (Figure 5A). DIO βCenpaKO mice demonstrated impaired glucose tolerance accompanied by reduced glucose-induced insulin secretion, and significantly decreased β-cell mitosis, proliferation, and mass in both males and females (Figure 5B, 5C, 5D, 5E, S5C). Furthermore, TUNEL-positive apoptotic β-cells were significantly increased in DIO βCenpaKO mice (Figure 5F). Since a glucose-mediated signal is essential for compensatory β-cell proliferation via insulin/IGF-1 signaling in DIO mice (Terauchi et al., 2007), we examined the role of CENP-A in the context of β-cell proliferation evoked by glucokinase activation. CENP-A deficient β-cells from βCenpaKO mice also demonstrated a significant decrease in cell proliferation in response to a glucokinase activator (Figure 5G). Although body weight gain was similar and blood

glucose levels were increased to similar levels in both groups by acute insulin resistance induced by an insulin receptor antagonist S961 (Schaffer et al., 2008), βCenpaKO mice exhibited a significant decrease in serum insulin levels, β-cell mass, mitosis, and proliferation compared with controls (Figure 5H, 5I, 5J, S5D, S5E). Thus, CENP-A plays an important role in the regulation of proliferation and the maintenance of β-cell mass in response to diverse physiological and pathophysiological demands.

The gene expression of CENP-A and PLK1 was enhanced in islets from control mice after S961 injection *in vivo* (Figure S5F **upper panel**). Furthermore, consistent with islet-specific effects of insulin on CENP-A and PLK1 expression (Figure S2H, S2I, S2J, S2K), we did not observe significant differences in gene expression of the M-phase proteins in liver or adipose tissues in S961-injected mice (Figure S5F, **lower panels**). To gain some insight into the mechanism(s) of action of S961 we examined the effect of exogenous insulin in the presence of S961 in control β cells *in vitro*. Presence of S961 abrogated the ability of exogenous insulin, but not exogenous IGF-1, to induce CENP-A and PLK1 expression *in vitro* (Figure S5G). One interpretation of these observations is that the β-cell proliferation induced by S961 injection *in vivo* is secondary to a systemic factor that acts via an insulin receptor-independent pathway. The source of this putative β-cell growth factor requires further investigation.

Role of CENP-A and PLK1 in β-cell proliferation and survival

To examine the direct role of CENP-A in cell cycle control we generated stable CENP-A-knockdown in control or in β-cell lines lacking proteins in the growth factor signaling pathway (e.g. IRS1KO, IRS2KO, or βIRKO) (Figure 6A, S6A). Assessment of EdU incorporation and an MTT assay, revealed that consistent with previous data (Folli et al., 2011) βIRKO cells showed decreased viability and metabolic activity compared with control, IRS1KO, or IRS2KO β-cells; and knockdown of CENP-A further reduced those activities in control, IRS1KO, or IRS2KO β-cells, but not in βIRKO cells (Figure 6B, 6C). Compared to scramble shRNA controls, CENP-A knockdown significantly increased G2/M-phase cells, suggesting G2/M cell cycle arrest (Figure 6D, S6B). Cyclin D plays a role in the G1/S phase transition, whereas cyclin B is a mitotic cyclin (Hochegger et al., 2008). The expression of cyclin B1, but not cyclin D2, is attenuated in CENP-A knockdown control β-cells in basal or cell cycle synchronized conditions (Figure 6E, S6C). The expression of Ki67, a proliferation marker, as well as CENP-A were elevated in *ob/ob* and LIRKO islets, two models which exhibit higher β-cell proliferation (Bock et al., 2003; El Ouaamari et al., 2016) (Figure 6F, 6G). Similar to the effects of CENP-A knockdown, PLK1 knockdown reduced cell proliferation in control and βIRKO β-cells as evaluated by both the MTT and EdU incorporation assays (Figure 6H, 6I, 6J). Further, inhibition of PLK1 with the PLK1-specific inhibitor BI-2536 (Steegmaier et al., 2007), prevented β-cell proliferation and G2/M cell cycle phase progression in a dose-dependent manner (Figure S6D, S6E, S6F). We next analyzed the ratio of necrotic propidium iodide (PI)-negative and apoptotic annexin V-positive cell populations to explore apoptosis. The treatment of control β-cells with the PLK1 inhibitor BI-2536 or the FoxM1 inhibitor thiostrepton significantly increased β-cell apoptosis (Figure 7A, S7A). Similarly, knockdown of CENP-A or PLK-1 in control β-cells demonstrated increased annexin V-positive apoptotic cells compared with scramble

knockdown cells (Figure 7B, S7B). Cleaved caspase-3 levels were significantly increased by knocking down CENP-A or PLK1 in control β-cells (Figure 7C). Interestingly, the expression of PLK1 was reduced in CENP-A knockdown cells, while conversely CENP-A expression was diminished in PLK1 knockdown cells (Figure 7C). We also confirmed that TUNEL-positive apoptotic β-cells were significantly increased in βCenpaKO mouse islets in response to chronic high glucose treatment (Figure 7D).

PLK1-dependent CENP-A deposition to centromere in β-cells

In mouse control β-cells, CENP-A deposition at the mouse centromere marker (minor satellite) was attenuated in both FoxM1 inhibitor treated control β-cells and intact βIRKO cells in ChIP analysis (Figure 7E). As well as CENP-A knockdown, PLK1 knockdown and treatment with the PLK1-specific inhibitor (BI-2536) repressed CENP-A binding at the centromere site (Figure 7F). The acetyl-Histone H3 binding to the β-actin promoter showed similar enrichment in all groups (Figure S7C, S7D). In human islets, CENP-A was recruited to the centromere site (α satellite) (Figure 7G). In independent experiments using the IR and IGF1R dual inhibitor, the PI3K inhibitor, or the PLK1 inhibitor, CENP-A binding to the centromere was reduced in human islets although acetyl-histone H3 binding to the internal control gene promoter was not modified by those inhibitors (Figure 7G, S7E). These data suggest that PLK1 is required for CENP-A deposition at the centromere in β-cells.

Discussion

Cell cycle progression in β-cells, similar to other mammalian cells, is controlled by a family of conserved cell cycle regulators. One attractive approach to increase β-cell mass in individuals with diabetes is to increase cell proliferation to generate functional insulin secreting cells. While most studies have focused on coaxing quiescent adult β-cells to progress though the G0/G1 checkpoint, it is possible that independent regulation of the M-phase is important for cells to complete mitosis. Here we report that regulation of the M-phase is critical for adaptive expansion of β-cell mass.

Among the proteins that regulate the M-phase we observed that CENP-A and PLK1 were up-regulated in models of islet hyperplasia such as the *ob/ob* and LIRKO mice (Bock et al., 2003; El Ouaamari et al., 2016; Okada et al., 2007) emphasizing their relevance in the β-cell adaptation to insulin resistance. Conversely, expression levels of CENP-A and PLK1 were significantly lower in a model that fails to compensate in response to high-fat diet-feeding (e.g. βIRKO) (Okada et al., 2007). The significance of CENP-A in the β-cell adaptive growth response was further supported when mice with a β-cell-specific KO of CENP-A were exposed to physiological states requiring adaptive compensation such as aging or pregnancy. In both cases significantly attenuated levels of pHH3+ mitotic β-cells indicated a compromised ability to compensate for ambient insulin resistance.

To examine the regulation of CENP-A we considered glucose and insulin both of which can modulate proteins in the growth factor signaling pathway (Assmann et al., 2009; Da Silva Xavier et al., 2004; Okada et al., 2007). While exogenous insulin and glucose both enhanced expression of CENP-A and PLK1 in wild type β-cells, glucose failed to show significant effects on CENP-A expression in β-cells lacking insulin receptors or in the presence of

diazoxide. The significance of insulin in regulating CENP-A was further confirmed when cells expressing a mutant ligand binding insulin receptor failed to mediate the effects of exogenous insulin on CENP-A expression.

CENP-A is poised for activation throughout the cell cycle but kept in an inactive non-centromeric state by Cdk1/2 activity during S, G2, and M phases (Silva et al., 2012). CENP-A is phosphorylated during early mitosis by Cdk1 and this phosphorylation is required for mitotic exit (Yu et al., 2015). Cdk1 also phosphorylates SPAT-1/Bora protein, a PLK1 activator, and regulates mitotic entry (Thomas et al., 2016). Thus Cdk activity is essential for proper cell cycle progression by regulating CENP-A and PLK1 activity. We observed that insulin-mediated CENP-A expression and deposition to the centromere is mediated by FoxM1 activation possibly through Cdk1/2. Importantly, the expression of FoxM1 was increased in *ob/ob* islets and the transcription factor has been reported to stimulate β-cell proliferation (Davis et al., 2010). Of relevance to our studies, FoxM1, CENP-A, and PLK1 expression have been reported to be elevated in islets of pancreatectomized mice which show increased β-cell proliferation (Ackermann Misfeldt et al., 2008). The decreased FoxM1 binding to CENP-A and PLK1 promoters in βIRKO β-cells was due to a reduction in insulin signaling and Cdk1/2 expression. Indeed, inhibition of PI3-kinase and Akt pathways induces G2/M arrest and apoptosis in HL60 cells while Akt promotes G2/M cell-cycle progression that is correlated with upregulation of Cdk1 expression in PC12 cells (Lee et al., 2005; Wang et al., 2009). Since FoxM1 is implicated in both G2/M-phase regulation and adaptive β-cell proliferation (Ackermann Misfeldt et al., 2008; Davis et al., 2010; Golson et al., 2015), targeting this transcription factor is one potential approach to enhance β-cell proliferation.

We are aware of previous studies reporting expression of human growth hormone in islets in MIP-Cre/ERT mice which could confound the interpretation of alterations in β-cell mass and glucose tolerance in gene-targeting experiments (Oropeza et al., 2015). However, in our study, the lack of difference in glucose tolerance and β-cell proliferation between the two control groups (MIP-Cre/ERT and CENP-A-floxed mice), and a *decrease* in β-cell mass in MIP-Cre/ERT;CENP-A-floxed (βCenpaKO) mice, coupled with direct effects of CENP-A knockdown in β-cells *in vitro*, suggests the phenotype in the βCenpaKO mice is due primarily to deficiency of CENP-A.

We also noted that the significant decrease in PLK1 when CENP-A was knocked down in the β-cell line was not evident in islets from βCenpaKO mice. This apparent difference between the *in vivo* and *in vitro* models may be related, in part, to the high cell proliferation generally observed in cell lines, which express high levels of PLK1, in contrast to very few cells progressing through the cell cycle *in vivo*. It is also possible that feedback effects potentially regulate each protein and this requires additional investigation.

Two observations argue for specificity of insulin effects on CENP-A and PLK1 in β-cells. First, we noted that modulating insulin receptors, either by addition of exogenous insulin or examining consequences of insulin receptor knockout, in hepatocytes or adipocytes (white and brown fat), had virtually no effect on the expression of CENP-A and PLK1. The specificity of insulin regulation of CENP-A and PLK1 could be related, in part, to

differential roles assigned to IRS proteins in metabolic cells. For example, IRS2 is important for β-cell proliferation (Kubota et al., 2004; Terauchi et al., 2007; Withers et al., 1999) while IRS-1 is linked to insulin secretion (Kulkarni et al., 1999b; Porzio et al., 1999). Whether similar differential signaling roles for IRS, or other adapter proteins, are linked to regulating cell cycle progression in other metabolic cell types requires further investigation. Second, we observed that S961 injection in control mice upregulated CENP-A and PLK1 expression in β-cells but not in other metabolic tissues (e.g. liver and white fat). Since CENP-A is required for S961-induced β-cell proliferation, it is possible that factors independent of insulin are able to modulate β-cell cycle control by regulating CENP-A expression. Potential signals include IGF1 receptors and ERK-mediated nuclear export of FoxO1 in βIRKO β cells (Mezza et al., 2016). The βIRKO mouse thus provides a useful model to explore whether the insulin receptor antagonist, S961, promotes proliferation independent of insulin receptors in β-cells.

In summary, we propose a model of insulin receptor-mediated regulation of proliferation and survival during the G2/M phase of the cell cycle in β-cells (Figure 7H). Upon stimulation with insulin, ERK facilitates FoxM1 localization to the nucleus, while PI3-kinase-mediated insulin signaling enhances FoxM1 binding to CENP-A and PLK1 promoters through Cdk1/2, leading to an increase in expression of CENP-A and PLK1. Subsequently, CENP-A deposition at the centromere is augmented by PLK1 to promote mitosis. In β-cells lacking insulin receptors or with poor expression of insulin signaling proteins, FoxM1 is localized to the nucleus due to constitutive activation of ERK. However, compromised insulin signaling inactivates FoxM1 in the nucleus leading to attenuated CENP-A expression and deposition at the centromere, mitotic arrest and apoptosis. These findings provide novel insights into the role of CENP-A in regulating G2/M cell cycle control with implications for β-cell loss secondary to poor cell cycle regulation in T2D.

STAR Methods

CONTACT FOR REAGENT AND RESOURCE SHARING

Further information and requests for resources and reagents should be directed to and will be fulfilled by the Lead Contact, Rohit N. Kulkarni MD PhD. (rohit.kulkarni@joslin.harvard.edu).

EXPERIMENTAL MODEL AND SUBJECT DETAILS

Cell lines—β-cell lines from control, IRS1KO, IRS2KO, or βIRKO mice were generated as described previously (Assmann et al., 2009; Kulkarni et al., 1999a). All β-cell lines were from male mice. The control cells were used between passages 11 to 21, IRS1KO and IRS2KO cells between passages 9 to 19 and βIRKO cells between passages 7 to 17. Cells were maintained in DMEM media containing 25 mM glucose, supplemented with 10% FBS. Experiments were performed using 80–90% confluent cells.

Mice—CENP-A floxed mice were generated from targeted C57BL/6 embryonic stem (ES) cells that were obtained from the European Conditional Mouse Mutagenesis Consortium (EUCOMM, $Cenpa^{tm1a(EUCOMM)Wtsi}$, EPD0445_6_E07). To obtain the Cenpa allele, the

mouse was crossed with the ROSA26::FLPe knock in mouse (B6.129S4-Gt(ROSA)26Sor$^{tm1(FLP1)Dym}$/RainJ) (Jackson Laboratories). MIP-cre/ERT mice (B6.Cg-Tg(Ins1-cre/ERT)1Lphi) were purchased from Jackson Laboratories. All mice were backcrossed for more than ten generations on the C57BL/6J background. β-cell-specific CENP-A deletion was generated by crossing CENP-A floxed mice with MIP-cre/ERT mice and tamoxifen administration at 7-weeks of age (intraperitoneal injection at a dose of 0.25 mg/g body weight, for a total of 3 doses over a 5-day period). Mice were injected with BrdU intraperitoneally (100 mg/kg body weight) 6 hours prior to animal sacrifice for immunostaining of the pancreas. The controls used throughout this paper are age-matched CENP-A floxed mice treated with tamoxifen. All protocols were approved by the Institutional Animal Care and Use Committee of the Joslin Diabetes Center and were in accordance with National Institutes of Health guidelines. All animals were housed in the Association for Assessment and Accreditation of Laboratory Animal Care International (AAALAC) accredited Animal Facility at Joslin Diabetes Center.

Human islet studies—Human islets were obtained from the Integrated Islet Distribution Program. Details of human islets are described in Table S4. All studies and protocols used were approved by the Joslin Diabetes Center's Committee on Human Studies (CHS#5-05). Upon receipt, islets were cultured overnight in Miami Media #1A (Cellgro). The islets were embedded in agarose and used for immunostaining studies. For the stimulation with insulin, the islets were starved in Final Wash/Culture Medium (Cellgro) for 5-hours before being stimulated with 10 nM insulin.

METHOD DETAILS

Cell culture experiments—β-cell lines were starved in DMEM media containing 2.8 mM glucose without serum for 12–16 hours. Cells were treated with 10 nM insulin (SIGMA), 10 nM IGF-1 (SIGMA), 200 nM OSI-906 (IR and IGF1R dual inhibitor, Med Chem express LLC), 1 μM S961 (insulin receptor antagonist), 50 μM LY294002 (PI3K inhibitor, Cell Signaling), 5 μM MK-2206 (Akt inhibitor, Cayman Chemical), 20 μM U0126 (MEK1/2 inhibitor, Cell Signaling), 50 nM BI-2536 (PLK1-specific inhibitor, Santa Cruz), or 10 μM thiostrepton (FoxM1 inhibitor, Santa Cruz).

Cell cycle synchronization—β-cell lines were synchronized at the G1–S boundary by double-thymidine block. Briefly, the cells were incubated for 18 hr in media containing 2 mM thymidine (Sigma) and then washed and incubated in thymidine-free media for 9 hr. They were re-incubated with thymidine for 16 hr. The cells were released from the block by adding fresh media without thymidine.

Cell cycle analysis—To evaluate the cell cycle distribution, the DNA content of the cells was assessed by flow cytometry. Briefly, the cells were fixed with cold 70% ethanol and stored at −20 °C for 2 hours, and then stained with PI/RNase staining buffer solution (BD Biosience, 550825). Cells were analyzed on an LSRII flow cytometer (BD Bioscience); we calculated the proportion of cells in G0/G1, S and G2/M phases using the FlowJo Ver.10 software. To detect M-phase-specific cells (prophase to anaphase), the cells were fixed and stained with Alexa 647-conjugated anti-phospho histone H3 (pS28) antibody (BD

Bioscience, 558217) with PI/RNase staining buffer solution. The proportion of M-phase cells among G2/M phase cells were analyzed using the FlowJo Ver.10 software.

Lentiviral transduction—Human wild type and S323L low-ligand binding mutant insulin receptor (IR) expression vectors were kindly provided by Jonathan Whittaker PhD (Case Western Reserve University, Cleveland, OH). Wild type and S323L IR open reading frames were cloned into pCDH-CMV-MCS-EF1-Puro lentiviral vector (System Biosciences). Lentivirus particles were generated by following the manufacturer's recommendation (Open Biosystems). Lentiviral particles for murine CENP-A short hairpin RNA (shRNA) (sc-37556-v), murine PLK1 shRNA (sc-36278-v), and control scramble shRNA (sc-108080) were purchased from Santa Cruz. Cells were infected by adding the lentiviral particles to the culture with polybrene (sc-134220). For generating stable cell lines, cells were treated with 4 mg/mL of puromycin 48 hours after the transduction and were maintained in selection media for more than 14 days. We generated two separate stable cell lines in each group.

Western Blotting—Cells, mouse islets, or human islets were solubilized in M-PER lysis buffer (Thermo Scientific #78501), liver tissue were solubilized in T-PER lysis buffer (Thermo Scientific #78510) with protease inhibitors and phosphatase inhibitors (Sigma P8340, P5726, P0044), and protein concentration was measured using a BCA protein assay kit (Pierce). The extracts were subjected to western blotting with primary antibodies overnight at 4°C. Mouse CENP-A (#2048), human CENP-A (#2186), PLK1 (#4535, #4513), pHH3 (#3377), insulin receptor β-subunit (#3025), IGF1R (#3027), phospho-IR/IGF1R (#3024), Akt (#9272), phospho-Akt (Ser473, #9271), β-actin (#4970), Cdk2 (#2546), Chk2 (#2662), ERK (#9102), p-ERK (Thr202/Tyr204 #4370), Cyclin B1 (#4138), Cyclin D2 (#3741), and cleaved caspase-3 (#9661) antibodies are from Cell Signaling. α-tubulin (ab7291), Lamin B1 (ab16048), and Cdk1 (ab32384) antibodies are from Abcam. Ki67 (M7187) antibody is from DAKO. FoxM1 (SC-502), PEPCK (sc-271029), and SREBP1 (sc-8984) antibodies are from Santa Cruz. Densitometry was performed using Image J software.

RNA isolation and quantitative RT-PCR—Total RNA was extracted using RNeasy Mini Kit (QIAGEN). One μg RNA was reverse-transcribed using a High-Capacity cDNA Reverse Transcription Kit (Applied Biosystems). Quantitative PCR was performed in an ABI 7900HT system, using SYBR Green Supermix (Bio-Rad). GAPDH or β-actin were used as an internal control. Primers described in Table. S2 were used for amplification.

Chromatin Immunoprecipitation (ChIP)—Chromatin was prepared from mouse β-cell lines and human islets. Briefly, β-cell cells or islets were fixed in 1% formaldehyde, and quenched in glycine. Cells were washed with PBS and lysed in cold lysis buffer with protease and phosphatase inhibitors (Sigma). Cells were then sonicated using 25% of power, 10-s on/off pulses for a total of 3 min (Branson digital sonifier). Immunoprecipitations were performed using control rabbit IgG (Cell Signaling #9649), anti-FoxM1 antibody (Santa Cruz, sc-502X), anti-mouse CENP-A antibody (Cell Signaling #2047), or anti-human CENP-A antibody (Abcam, ab33565). The ChIP qPCR was performed with the primers described in Table S3.

Mouse studies—Because tamoxifen is known to affect β-cell proliferation during pregnancy (Roshangar et al., 2010) and pregnancy rates appear to be poor after tamoxifen injection, inter-breeding of mice was performed at 6 weeks after last tamoxifen injection for the pregnancy study. Eight-week old mice were fed with high-fat diet (Research Diet, catalog# D12492) for 16 weeks to create a model of diet-induced obesity. For S961 studies, 9–11-week-old mice were anesthetized and infused with PBS alone or PBS with the insulin receptor antagonist S961 at the dose of 10 nmoles/week for 8 days. Infusion was carried out using osmotic pumps (ALZET) implanted subcutaneously.

The blood glucose and plasma insulin levels were determined using a Contour blood glucose meter (Bayer Health Care), and an insulin ELISA kit (Crystal Chem Inc.), respectively. An insulin tolerance test was performed by intraperitoneal injection with human insulin (0.75 mU/g body weight for normal chow-fed mice, 1.5 mU/g body weight for high-fat diet-fed mice). An intraperitoneal glucose tolerance test was performed by withholding all food from the mice for more than 14 hours and then intraperitoneally loading the mice with glucose (1.5 mg/g body weight).

Immunostaining studies—Mouse pancreases, dispersed mouse islets, in vitro cultured human islets were analyzed by immunostaining using anti-insulin (Abcam, ab7842), anti-BrdU (Dako, m0744), anti-phospho-histone H3 (pHH3) (EMD Millipore, 06-570), anti-mouse-CENP-A (Cell Signaling #2048), anti-human CENP-A (Cell Signaling, #2186), anti-PLK1 (Thermo Scientific, 36-298), anti-FoxM1 (Abcam, ab175798), or anti-Cre (Novagen, 69050-3) antibodies. Cell counting was manually performed in a blinded fashion by a single observer. BrdU+ or Ki67+ β-cells were assessed by confocal microscopy (LSM-7 DUO, Carl Zeiss). Insulin+ cells showing nuclear DAPI staining were considered as β-cells. Insulin+ cells showing nuclear colocalized staining for DAPI+ and pHH3+ or BrdU+ were counted as mitotic or proliferating β-cells. At least 1000 β-cells per mouse were analyzed. The proportion of the area of pancreatic tissue occupied by the β-cells was calculated using Image J software.

Mouse islet studies—Islets were isolated from 8–12 weeks old wild type C57BL/6 male mice, CENP-A-floxed mice, or MIP-cre/ERT;CENP-A floxed mice using intraductal collagenase technique (Shirakawa et al., 2013). Islets were handpicked and cultured overnight in RPMI 1640 media containing 5 mM glucose and 10% fetal bovine serum (FBS). For glucose-stimulated insulin secretion from islets, ten islets were incubated at 37°C for 1.5 hours in Krebs-Ringer bicarbonate buff er containing 2.8mM, 11.1mM, or 16.7 mM glucose after pre-incubation with 2.8mM glucose for 1.5 hours. The islets were extracted with acid ethanol. The insulin concentration of the assay buffer and the insulin content were measured using an insulin ELISA kit (Crystal Chem Inc.). For studies related to stimulation with insulin, islets were subjected to 6h-starvation in RPMI 1640 media containing 3 mM glucose and 0.1%BSA, followed by stimulation as shown. Glucokinase activator Cpd A (2-amino-5-(4-methyl-4H-(1,2,4)-triazole-3-yl-sulfanyl)-N-(4-methyl-thiazole-2-yl)benzamide), was purchased from Calbiochem.

Analysis of cell proliferation and apoptosis—For a modified MTT assay, cells were plated in 96-well plates @ 10^4 cells in each well. The cell number was determined using the

CellTiter 96 Non-Radioactive Cell Proliferation Assay (Promega, G4001) according to the manufacturer's instructions. For EdU incorporation assay, cells were treated with 10 μm EdU (4h) and stained with Click-iT Plus EdU Alexa Fluor 488 or 594 Imaging Kit (Thermo Fisher, C10637, C10639). Apoptosis was measured by Annexin V and PI staining using an Annexin V-FITC Apoptosis kit (Sigma). Cells were stained according to the manufacturer's instructions and processed for flow cytometry (LSRII, BD). TUNEL staining was performed in vivo or in vitro using the ApopTag Fluorescein In Situ Apoptosis Detection Kit or ApopTag Red In Situ Apoptosis Detection Kit (EMD Millipore). For TUNEL staining, at least 100 islets per mouse (in vivo) or 1000 cells group (in vitro) attached to poly-L-lysine coated coverslips (Falcon) were analyzed using the LSM7 DUO confocal laser scanning microscope (Carl Zeiss) to assess the proportion of immunostained nuclei among the insulin-positive cells.

Inclusion and exclusion criteria—No inclusion and exclusion criteria were applied to the data collection or the subject selection in this study.

QUANTIFICATION AND STATISTICAL ANALYSIS

Statistics—All experiments were independently repeated at least three times. Results are shown as means ± SE. Statistical analyses were conducted using Prism 7 software (GraphPad Software). Gaussian distribution was determined by using a D'Agostino-Pearson test. Statistical comparisons between groups were analyzed for significance by an unpaired two-tailed Student's t-test and one-way analysis of variance (ANOVA) with post-hoc Tukey tests for a parametric test, or Mann-Whitney U test for a nonparametric test. Differences are considered significant at $p < 0.05$. The exact values of n, statistical measures (mean ± SE) and statistical significance are reported in the figures and in the figure legends.

Supplementary Material

Refer to Web version on PubMed Central for supplementary material.

Acknowledgments

We thank C. Ronald Kahn MD (Joslin Diabetes Center, Boston, MA) for tissues from the FIRKO mice, Matthew D. Lynes PhD and Yu-Hua Tseng PhD (Joslin Diabetes Center, Boston, MA) for tissues from Myf5IRKO mice, and Maureen A. Gannon PhD (Vanderbilt University Medical Center, Nashville, TN) for discussions on FoxM1. Human wild type and S323L low-ligand binding mutant insulin receptor (IR) expression vectors were provided by Jonathan Whittaker PhD (Case Western Reserve University, Cleveland, OH). S961 compound was a kind gift from Lauge Schaffer (Novo Nordisk). This work was primarily supported by NIH RO1 DK67536 (R.N.K.), and in part by RO1 DK103215 and UC4 DK104167 (to R.N.K.). J.S. is supported by a Post-Doctoral Fellowship for Research Abroad, the Japan Society for the Promotion of Science (JSPS) and the Uehara Memorial Foundation. A.E. is supported by JDRF Advanced Postdoctoral Fellowship (3-APF-2014-182-A-N).

References

Ackermann Misfeldt A, Costa RH, Gannon M. Beta-cell proliferation, but not neogenesis, following 60% partial pancreatectomy is impaired in the absence of FoxM1. Diabetes. 2008; 57:3069–3077. [PubMed: 18728229]

Assmann A, Ueki K, Winnay JN, Kadowaki T, Kulkarni RN. Glucose effects on beta-cell growth and survival require activation of insulin receptors and insulin receptor substrate 2. Mol Cell Biol. 2009; 29:3219–3228. [PubMed: 19273608]

Bernal-Mizrachi E, Fatrai S, Johnson JD, Ohsugi M, Otani K, Han Z, Polonsky KS, Permutt MA. Defective insulin secretion and increased susceptibility to experimental diabetes are induced by reduced Akt activity in pancreatic islet beta cells. The Journal of clinical investigation. 2004; 114:928–936. [PubMed: 15467831]

Bluher M, Michael MD, Peroni OD, Ueki K, Carter N, Kahn BB, Kahn CR. Adipose tissue selective insulin receptor knockout protects against obesity and obesity-related glucose intolerance. Dev Cell. 2002; 3:25–38. [PubMed: 12110165]

Bock T, Pakkenberg B, Buschard K. Increased islet volume but unchanged islet number in ob/ob mice. Diabetes. 2003; 52:1716–1722. [PubMed: 12829638]

Bruinsma W, Raaijmakers JA, Medema RH. Switching Polo-like kinase-1 on and off in time and space. Trends Biochem Sci. 2012; 37:534–542. [PubMed: 23141205]

Da Silva Xavier G, Qian Q, Cullen PJ, Rutter GA. Distinct roles for insulin and insulin-like growth factor-1 receptors in pancreatic beta-cell glucose sensing revealed by RNA silencing. The Biochemical journal. 2004; 377:149–158. [PubMed: 14563207]

Davis DB, Lavine JA, Suhonen JI, Krautkramer KA, Rabaglia ME, Sperger JM, Fernandez LA, Yandell BS, Keller MP, Wang IM, Schadt EE, Attie AD. FoxM1 is up-regulated by obesity and stimulates beta-cell proliferation. Mol Endocrinol. 2010; 24:1822–1834. [PubMed: 20660304]

Demozay D, Tsunekawa S, Briaud I, Shah R, Rhodes CJ. Specific glucose-induced control of insulin receptor substrate-2 expression is mediated via Ca2+-dependent calcineurin/NFAT signaling in primary pancreatic islet beta-cells. Diabetes. 2011; 60:2892–2902. [PubMed: 21940781]

Dhawan S, Dirice E, Kulkarni RN, Bhushan A. Inhibition of TGF-beta Signaling Promotes Human Pancreatic beta-Cell Replication. Diabetes. 2016; 65:1208–1218. [PubMed: 26936960]

DiPaola RS. To arrest or not to G(2)-M Cell-cycle arrest: commentary re: A. K. Tyagi et al., Silibinin strongly synergizes human prostate carcinoma DU145 cells to doxorubicin-induced growth inhibition, G(2)-M arrest, and apoptosis. Clin cancer res. 2002; 8:3512–3519. [PubMed: 12429642] Clin Cancer Res. 2002; 8:3311–3314. [PubMed: 12429616]

Dirice E, Walpita D, Vetere A, Meier BC, Kahraman S, Hu J, Dancik V, Burns SM, Gilbert TJ, Olson DE, Clemons PA, Kulkarni RN, Wagner BK. Inhibition of DYRK1A Stimulates Human beta-Cell Proliferation. Diabetes. 2016; 65:1660–1671. [PubMed: 26953159]

El Ouaamari A, Dirice E, Gedeon N, Hu J, Zhou JY, Shirakawa J, Hou L, Goodman J, Karampelias C, Qiang G, Boucher J, Martinez R, Gritsenko MA, De Jesus DF, Kahraman S, Bhatt S, Smith RD, Beer HD, Jungtrakoon P, Gong Y, Goldfine AB, Liew CW, Doria A, Andersson O, Qian WJ, Remold-O'Donnell E, Kulkarni RN. SerpinB1 Promotes Pancreatic beta Cell Proliferation. Cell Metab. 2016; 23:194–205. [PubMed: 26701651]

Fiaschi-Taesch NM, Kleinberger JW, Salim FG, Troxell R, Wills R, Tanwir M, Casinelli G, Cox AE, Takane KK, Scott DK, Stewart AF. Human pancreatic beta-cell G1/S molecule cell cycle atlas. Diabetes. 2013; 62:2450–2459. [PubMed: 23493570]

Folli F, Okada T, Perego C, Gunton J, Liew CW, Akiyama M, D'Amico A, La Rosa S, Placidi C, Lupi R, Marchetti P, Sesti G, Hellerstein M, Perego L, Kulkarni RN. Altered insulin receptor signalling and beta-cell cycle dynamics in type 2 diabetes mellitus. PLoS One. 2011; 6:e28050. [PubMed: 22140505]

Foltz DR, Jansen LE, Black BE, Bailey AO, Yates JR 3rd, Cleveland DW. The human CENP-A centromeric nucleosome-associated complex. Nat Cell Biol. 2006; 8:458–469. [PubMed: 16622419]

Golson ML, Dunn JC, Maulis MF, Dadi PK, Osipovich AB, Magnuson MA, Jacobson DA, Gannon M. Activation of FoxM1 Revitalizes the Replicative Potential of Aged beta-Cells in Male Mice and Enhances Insulin Secretion. Diabetes. 2015; 64:3829–3838. [PubMed: 26251404]

Gunton JE, Kulkarni RN, Yim S, Okada T, Hawthorne WJ, Tseng YH, Roberson RS, Ricordi C, O'Connell PJ, Gonzalez FJ, Kahn CR. Loss of ARNT/HIF1beta mediates altered gene expression and pancreatic-islet dysfunction in human type 2 diabetes. Cell. 2005; 122:337–349. [PubMed: 16096055]

Hayes HL, Zhang L, Becker TC, Haldeman JM, Stephens SB, Arlotto M, Moss LG, Newgard CB, Hohmeier HE. A Pdx-1-Regulated Soluble Factor Activates Rat and Human Islet Cell Proliferation. Mol Cell Biol. 2016; 36:2918–2930. [PubMed: 27620967]

Hegde NS, Sanders DA, Rodriguez R, Balasubramanian S. The transcription factor FOXM1 is a cellular target of the natural product thiostrepton. Nat Chem. 2011; 3:725–731. [PubMed: 21860463]

Hochegger H, Takeda S, Hunt T. Cyclin-dependent kinases and cell-cycle transitions: does one fit all? Nat Rev Mol Cell Biol. 2008; 9:910–916. [PubMed: 18813291]

Kang YH, Park JE, Yu LR, Soung NK, Yun SM, Bang JK, Seong YS, Yu H, Garfield S, Veenstra TD, Lee KS. Self-regulated Plk1 recruitment to kinetochores by the Plk1-PBIP1 interaction is critical for proper chromosome segregation. Mol Cell. 2006; 24:409–422. [PubMed: 17081991]

Kondegowda NG, Fenutria R, Pollack IR, Orthofer M, Garcia-Ocana A, Penninger JM, Vasavada RC. Osteoprotegerin and Denosumab Stimulate Human Beta Cell Proliferation through Inhibition of the Receptor Activator of NF-kappaB Ligand Pathway. Cell Metab. 2015; 22:77–85. [PubMed: 26094891]

Kubota N, Terauchi Y, Tobe K, Yano W, Suzuki R, Ueki K, Takamoto I, Satoh H, Maki T, Kubota T, Moroi M, Okada-Iwabu M, Ezaki O, Nagai R, Ueta Y, Kadowaki T, Noda T. Insulin receptor substrate 2 plays a crucial role in beta cells and the hypothalamus. The Journal of clinical investigation. 2004; 114:917–927. [PubMed: 15467830]

Kulkarni RN, Bruning JC, Winnay JN, Postic C, Magnuson MA, Kahn CR. Tissue-specific knockout of the insulin receptor in pancreatic beta cells creates an insulin secretory defect similar to that in type 2 diabetes. Cell. 1999a; 96:329–339. [PubMed: 10025399]

Kulkarni RN, Holzenberger M, Shih DQ, Ozcan U, Stoffel M, Magnuson MA, Kahn CR. beta-cell-specific deletion of the Igf1 receptor leads to hyperinsulinemia and glucose intolerance but does not alter beta-cell mass. Nat Genet. 2002; 31:111–115. [PubMed: 11923875]

Kulkarni RN, Winnay JN, Daniels M, Bruning JC, Flier SN, Hanahan D, Kahn CR. Altered function of insulin receptor substrate-1-deficient mouse islets and cultured beta-cell lines. The Journal of clinical investigation. 1999b; 104:R69–75. [PubMed: 10606633]

Lee SH, Itkin-Ansari P, Levine F. CENP-A, a protein required for chromosome segregation in mitosis, declines with age in islet but not exocrine cells. Aging (Albany NY). 2010; 2:785–790. [PubMed: 21068465]

Lee SR, Park JH, Park EK, Chung CH, Kang SS, Bang OS. Akt-induced promotion of cell-cycle progression at G2/M phase involves upregulation of NF-Y binding activity in PC12 cells. J Cell Physiol. 2005; 205:270–277. [PubMed: 15887249]

Lynes MD, Schulz TJ, Pan AJ, Tseng YH. Disruption of insulin signaling in Myf5-expressing progenitors leads to marked paucity of brown fat but normal muscle development. Endocrinology. 2015; 156:1637–1647. [PubMed: 25625589]

Major ML, Lepe R, Costa RH. Forkhead box M1B transcriptional activity requires binding of Cdk-cyclin complexes for phosphorylation-dependent recruitment of p300/CBP coactivators. Mol Cell Biol. 2004; 24:2649–2661. [PubMed: 15024056]

McKinley KL, Cheeseman IM. Polo-like kinase 1 licenses CENP-A deposition at centromeres. Cell. 2014; 158:397–411. [PubMed: 25036634]

Meier JJ, Butler AE, Saisho Y, Monchamp T, Galasso R, Bhushan A, Rizza RA, Butler PC. Beta-cell replication is the primary mechanism subserving the postnatal expansion of beta-cell mass in humans. Diabetes. 2008; 57:1584–1594. [PubMed: 18334605]

Mezza T, Shirakawa J, Martinez R, Hu J, Giaccari A, Kulkarni RN. Nuclear Export of FoxO1 Is Associated with ERK Signaling in beta-Cells Lacking Insulin Receptors. J Biol Chem. 2016; 291:21485–21495. [PubMed: 27535223]

Michael MD, Kulkarni RN, Postic C, Previs SF, Shulman GI, Magnuson MA, Kahn CR. Loss of insulin signaling in hepatocytes leads to severe insulin resistance and progressive hepatic dysfunction. Mol Cell. 2000; 6:87–97. [PubMed: 10949030]

Muller D, Huang GC, Amiel S, Jones PM, Persaud SJ. Identification of insulin signaling elements in human beta-cells: autocrine regulation of insulin gene expression. Diabetes. 2006; 55:2835–2842. [PubMed: 17003350]

Okada T, Liew CW, Hu J, Hinault C, Michael MD, Krtzfeldt J, Yin C, Holzenberger M, Stoffel M, Kulkarni RN. Insulin receptors in beta-cells are critical for islet compensatory growth response to insulin resistance. Proc Natl Acad Sci U S A. 2007; 104:8977–8982. [PubMed: 17416680]

Oropeza D, Jouvet N, Budry L, Campbell JE, Bouyakdan K, Lacombe J, Perron G, Bergeron V, Neuman JC, Brar HK, Fenske RJ, Meunier C, Sczelecki S, Kimple ME, Drucker DJ, Screaton RA, Poitout V, Ferron M, Alquier T, Estall JL. Phenotypic Characterization of MIP-CreERT1Lphi Mice With Transgene-Driven Islet Expression of Human Growth Hormone. Diabetes. 2015; 64:3798–3807. [PubMed: 26153246]

Park CH, Park JE, Kim TS, Kang YH, Soung NK, Zhou M, Kim NH, Bang JK, Lee KS. Mammalian Polo-like kinase 1 (Plk1) promotes proper chromosome segregation by phosphorylating and delocalizing the PBIP1.CENP-Q complex from kinetochores. J Biol Chem. 2015; 290:8569–8581. [PubMed: 25670858]

Porzio O, Federici M, Hribal ML, Lauro D, Accili D, Lauro R, Borboni P, Sesti G. The Gly972-->Arg amino acid polymorphism in IRS-1 impairs insulin secretion in pancreatic beta cells. The Journal of clinical investigation. 1999; 104:357–364. [PubMed: 10430617]

Prudente S, Jungtrakoon P, Marucci A, Ludovico O, Buranasupkajorn P, Mazza T, Hastings T, Milano T, Morini E, Mercuri L, Bailetti D, Mendonca C, Alberico F, Basile G, Romani M, Miccinilli E, Pizzuti A, Carella M, Barbetti F, Pascarella S, Marchetti P, Trischitta V, Di Paola R, Doria A. Loss-of-Function Mutations in APPL1 in Familial Diabetes Mellitus. American journal of human genetics. 2015; 97:177–185. [PubMed: 26073777]

Rahier J, Guiot Y, Goebbels RM, Sempoux C, Henquin JC. Pancreatic beta-cell mass in European subjects with type 2 diabetes. Diabetes Obes Metab. 2008; 10(Suppl 4):32–42. [PubMed: 18834431]

Regnier V, Vagnarelli P, Fukagawa T, Zerjal T, Burns E, Trouche D, Earnshaw W, Brown W. CENP-A is required for accurate chromosome segregation and sustained kinetochore association of BubR1. Mol Cell Biol. 2005; 25:3967–3981. [PubMed: 15870271]

Roach P, Zick Y, Formisano P, Accili D, Taylor SI, Gorden P. A novel human insulin receptor gene mutation uniquely inhibits insulin binding without impairing posttranslational processing. Diabetes. 1994; 43:1096–1102. [PubMed: 8070609]

Roshangar L, Rad JS, Afsordeh K. Maternal tamoxifen treatment alters oocyte differentiation in the neonatal mice: inhibition of oocyte development and decreased folliculogenesis. J Obstet Gynaecol Res. 2010; 36:224–231. [PubMed: 20492370]

Schaffer L, Brand CL, Hansen BF, Ribel U, Shaw AC, Slaaby R, Sturis J. A novel high-affinity peptide antagonist to the insulin receptor. Biochemical and biophysical research communications. 2008; 376:380–383. [PubMed: 18782558]

Shelby RD, Vafa O, Sullivan KF. Assembly of CENP-A into centromeric chromatin requires a cooperative array of nucleosomal DNA contact sites. J Cell Biol. 1997; 136:501–513. [PubMed: 9024683]

Shirakawa J, Kulkarni RN. Novel factors modulating human beta-cell proliferation. Diabetes Obes Metab. 2016; 18(Suppl 1):71–77. [PubMed: 27615134]

Shirakawa J, Togashi Y, Sakamoto E, Kaji M, Tajima K, Orime K, Inoue H, Kubota N, Kadowaki T, Terauchi Y. Glucokinase activation ameliorates ER stress-induced apoptosis in pancreatic beta-cells. Diabetes. 2013; 62:3448–3458. [PubMed: 23801577]

Silva MC, Bodor DL, Stellfox ME, Martins NM, Hochegger H, Foltz DR, Jansen LE. Cdk activity couples epigenetic centromere inheritance to cell cycle progression. Dev Cell. 2012; 22:52–63. [PubMed: 22169070]

Steegmaier M, Hoffmann M, Baum A, Lenart P, Petronczki M, Krssak M, Gurtler U, Garin-Chesa P, Lieb S, Quant J, Grauert M, Adolf GR, Kraut N, Peters JM, Rettig WJ. BI 2536, a potent and selective inhibitor of polo-like kinase 1, inhibits tumor growth in vivo. Curr Biol. 2007; 17:316–322. [PubMed: 17291758]

Tan Y, Raychaudhuri P, Costa RH. Chk2 mediates stabilization of the FoxM1 transcription factor to stimulate expression of DNA repair genes. Mol Cell Biol. 2007; 27:1007–1016. [PubMed: 17101782]

Terauchi Y, Takamoto I, Kubota N, Matsui J, Suzuki R, Komeda K, Hara A, Toyoda Y, Miwa I, Aizawa S, Tsutsumi S, Tsubamoto Y, Hashimoto S, Eto K, Nakamura A, Noda M, Tobe K, Aburatani H, Nagai R, Kadowaki T. Glucokinase and IRS-2 are required for compensatory beta cell hyperplasia in response to high-fat diet-induced insulin resistance. The Journal of clinical investigation. 2007; 117:246–257. [PubMed: 17200721]

Thomas Y, Cirillo L, Panbianco C, Martino L, Tavernier N, Schwager F, Van Hove L, Joly N, Santamaria A, Pintard L, Gotta M. Cdk1 Phosphorylates SPAT-1/Bora to Promote Plk1 Activation in C. elegans and Human Cells. Cell Rep. 2016; 15:510–518. [PubMed: 27068477]

Wang IC, Chen YJ, Hughes D, Petrovic V, Major ML, Park HJ, Tan Y, Ackerson T, Costa RH. Forkhead box M1 regulates the transcriptional network of genes essential for mitotic progression and genes encoding the SCF (Skp2-Cks1) ubiquitin ligase. Mol Cell Biol. 2005; 25:10875–10894. [PubMed: 16314512]

Wang J, Wu A, Xu Y, Liu J, Qian X. M(2)-A induces apoptosis and G(2)-M arrest via inhibiting PI3K/Akt pathway in HL60 cells. Cancer Lett. 2009; 283:193–202. [PubMed: 19435648]

Wang P, Alvarez-Perez JC, Felsenfeld DP, Liu H, Sivendran S, Bender A, Kumar A, Sanchez R, Scott DK, Garcia-Ocana A, Stewart AF. A high-throughput chemical screen reveals that harmine-mediated inhibition of DYRK1A increases human pancreatic beta cell replication. Nat Med. 2015; 21:383–388. [PubMed: 25751815]

Wicksteed B, Brissova M, Yan W, Opland DM, Plank JL, Reinert RB, Dickson LM, Tamarina NA, Philipson LH, Shostak A, Bernal-Mizrachi E, Elghazi L, Roe MW, Labosky PA, Myers MG Jr, Gannon M, Powers AC, Dempsey PJ. Conditional gene targeting in mouse pancreatic ss-Cells: analysis of ectopic Cre transgene expression in the brain. Diabetes. 2010; 59:3090–3098. [PubMed: 20802254]

Withers DJ, Burks DJ, Towery HH, Altamuro SL, Flint CL, White MF. Irs-2 coordinates Igf-1 receptor-mediated beta-cell development and peripheral insulin signalling. Nat Genet. 1999; 23:32–40. [PubMed: 10471495]

Xuan S, Kitamura T, Nakae J, Politi K, Kido Y, Fisher PE, Morroni M, Cinti S, White MF, Herrera PL, Accili D, Efstratiadis A. Defective insulin secretion in pancreatic beta cells lacking type 1 IGF receptor. The Journal of clinical investigation. 2002; 110:1011–1019. [PubMed: 12370279]

Yu Z, Zhou X, Wang W, Deng W, Fang J, Hu H, Wang Z, Li S, Cui L, Shen J, Zhai L, Peng S, Wong J, Dong S, Yuan Z, Ou G, Zhang X, Xu P, Lou J, Yang N, Chen P, Xu RM, Li G. Dynamic phosphorylation of CENP-A at Ser68 orchestrates its cell-cycle-dependent deposition at centromeres. Dev Cell. 2015; 32:68–81. [PubMed: 25556658]

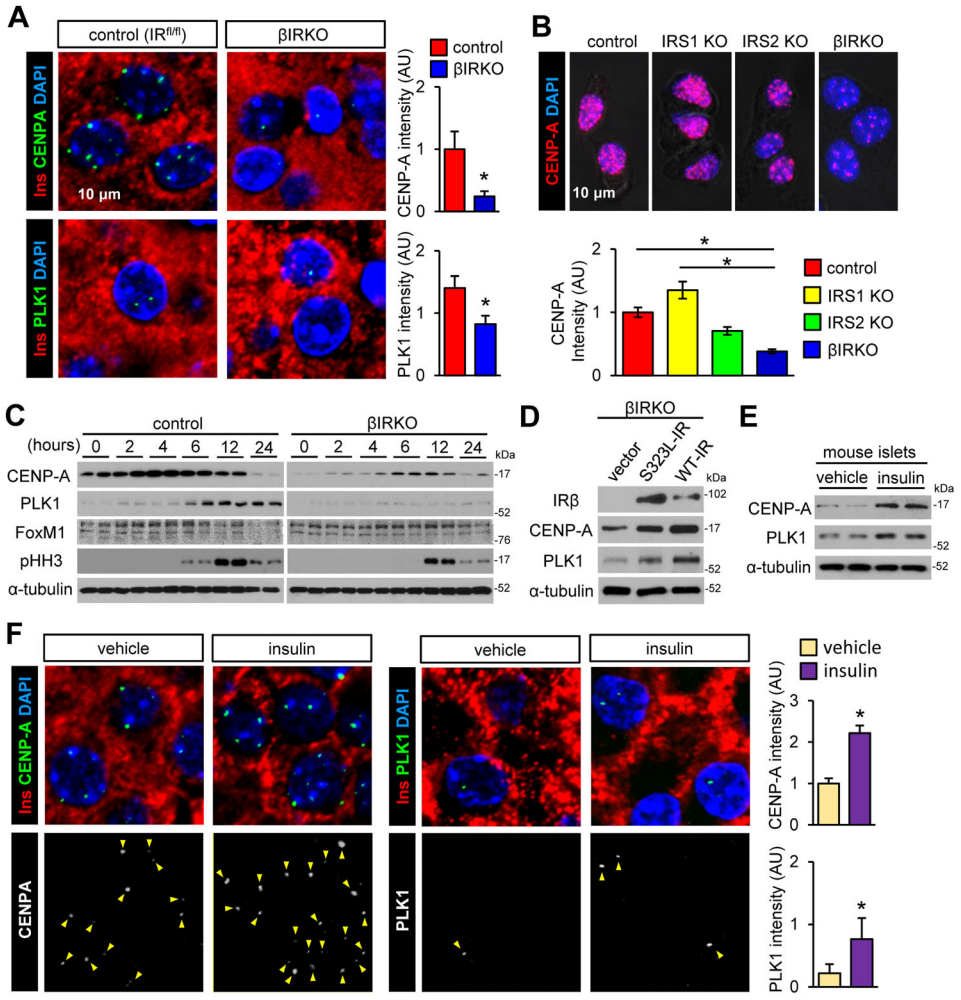

Figure 1. Insulin receptor-mediated CENP-A and PLK1 expression in β-cells

(A) Left panel; Representative images immunostained for CENP-A or PLK1, insulin and DAPI from endocrine pancreas of control and βIRKO mice. Right panel; Quantification of CENP-A or PLK1 fluorescence in insulin$^+$ cells. *$p < 0.05$ (n=5).

(B) Upper panel; Representative images immunostained for CENP-A and DAPI from indicated β-cell lines. Lower panel; Quantification of CENP-A in each β-cell line. *$p < 0.05$ (n=5).

(C) Western blot of indicated proteins in control and βIRKO β-cell lines after cell cycle synchronization by double thymidine block.

(D) Western blot of indicated proteins in βIRKO β-cells transduced with wild-type insulin receptor (IR), S323L low insulin-binding mutant IR, or vector.

(E) Western blot of indicated proteins in 8 week-old male control mouse islets stimulated with 100 nM insulin for 12 hours.

(F) Left panel; Representative images immunostained for CENP-A or PLK1, insulin and DAPI from embedded islets of control mice stimulated with 100 nM insulin for 24 hours. Right panel; Quantification of CENP-A or PLK1 fluorescence in insulin$^+$ cells. *$p < 0.05$ (n=4).

All data are represented as mean ± SEM in (A), (B), and (F).
See also Figure S1.

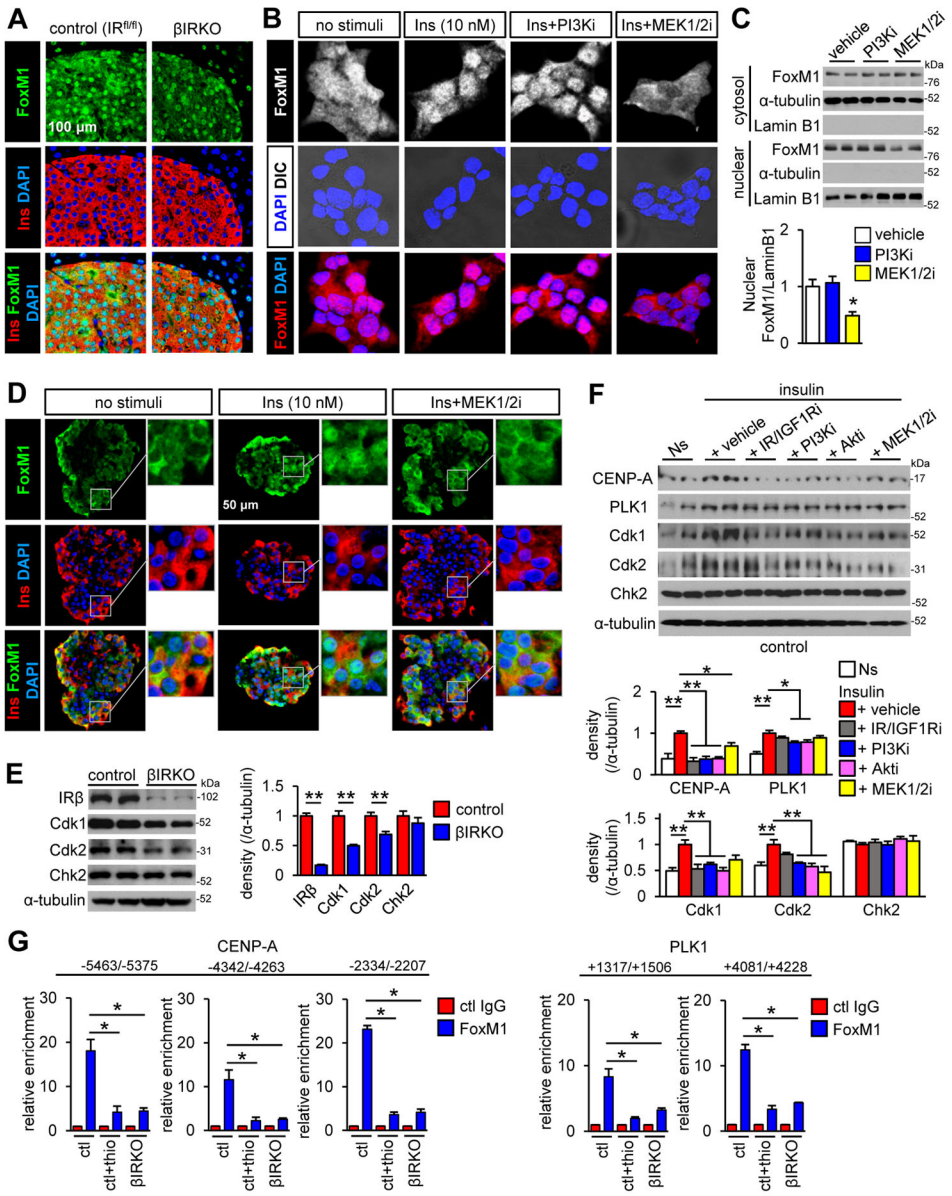

Figure 2. FoxM1 binding to CENP-A and PLK1-associated DNA is facilitated by insulin receptor-mediated signals

(A) Representative images immunostained for FoxM1, insulin, and DAPI from endocrine pancreas of control and βIRKO mice.

(B) Representative images immunostained for FoxM1 and DAPI from control β-cell line in the presence or absence of 10 nM insulin, 50 μM LY294002 (PI3Ki), or 20 μM U0126 (MEKi) for 3 hours.

(C) Upper panel; Nuclear cytoplasmic fractionation and western blot of FoxM1 in control β-cells in the presence or absence of 50 μM LY294002 (PI3Ki) or 20 μM U0126 (MEKi) for 12 hours. α-tubulin is cytosolic marker and Lamin B1 is nuclear marker. Lower panel; Intensity of the signals quantified by densitometry. *p < 0.05 (n=4).

(D) Representative images immunostained for FoxM1, insulin, and DAPI of human islets from non-diabetes donor in the presence or absence of 10 nM insulin or 20 μM U0126 (MEKi) for 6 hours. For details of the human donors please see Table S4.
(E) Left panel; Western blot of indicated proteins in control and βIRKO β-cells. Right panel; Intensity of the signals quantified by densitometry. **$p < 0.01$ (n=4).
(F) Upper panel; Western blot of indicated proteins in control β-cells in the presence of 10 nM insulin, 200 nM OSI-906 (IR/IGF1Ri), 50 μM LY294002 (PI3Ki), 5 μM MK-2206 (Akti), or 20 μM U0126 (MEKi) for 24 hours. Lower panel; Intensity of the signals quantified by densitometry. *$p < 0.05$, **$p < 0.01$ (n=4).
(G) ChIP assays for FoxM1 on CENP-A or PLK1 genomic regions in control β-cells in the presence of 10 μM thiostrepton for 24 hours or in βIRKO β-cells. *$p < 0.05$ (n=5).
All data are represented as mean ± SEM in (C) and (E–G).
See also Figure S2.

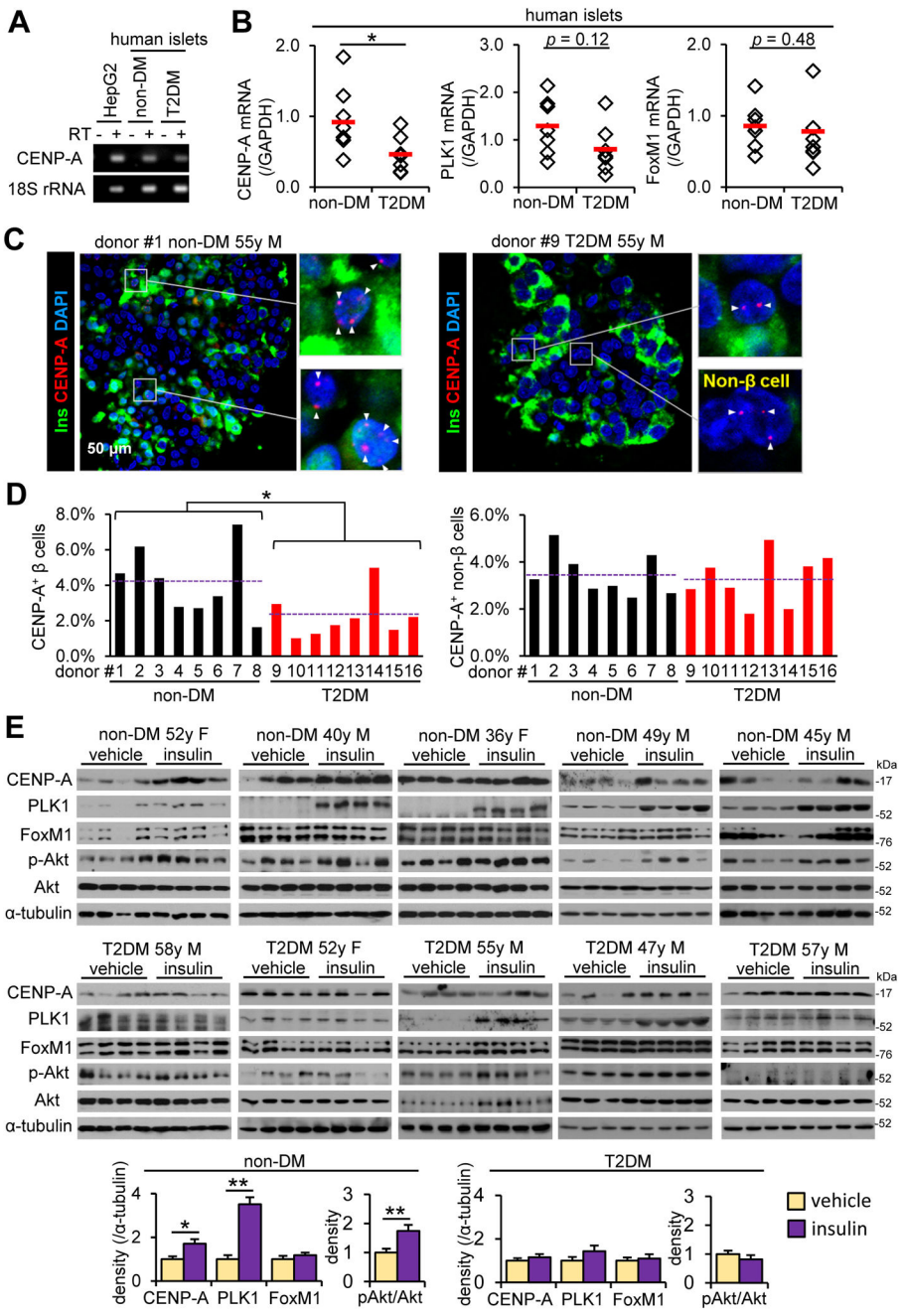

Figure 3. Insulin-induced CENP-A expression in human islets is impaired in type 2 diabetes

(A) Reverse Transcription (RT)-PCR analysis of human islets and HepG2 cells.

(B) Quantitative RT-PCR analysis of human islets from non-diabetes and type 2 diabetes donors. *p < 0.05 (n=7).

(C) Representative images immunostained for CENP-A, insulin and DAPI from human islets of non-diabetes and type 2 diabetes donor.

(D) Quantification of CENP-A+ insulin+ β-cells and CENP-A+ insulin- non-β-cells in each human islets. *p < 0.05 (n=5).

(E) Upper panel; Western blot of indicated proteins in human islets stimulated with 100 nM insulin for 24 hours. Lower panel; Intensity of the signals quantified by densitometry. Data are represented as mean ± SEM. *$p < 0.05$, **$p < 0.01$ (n=5).
For details of the human donors please see Table S4.
See also Figure S3.

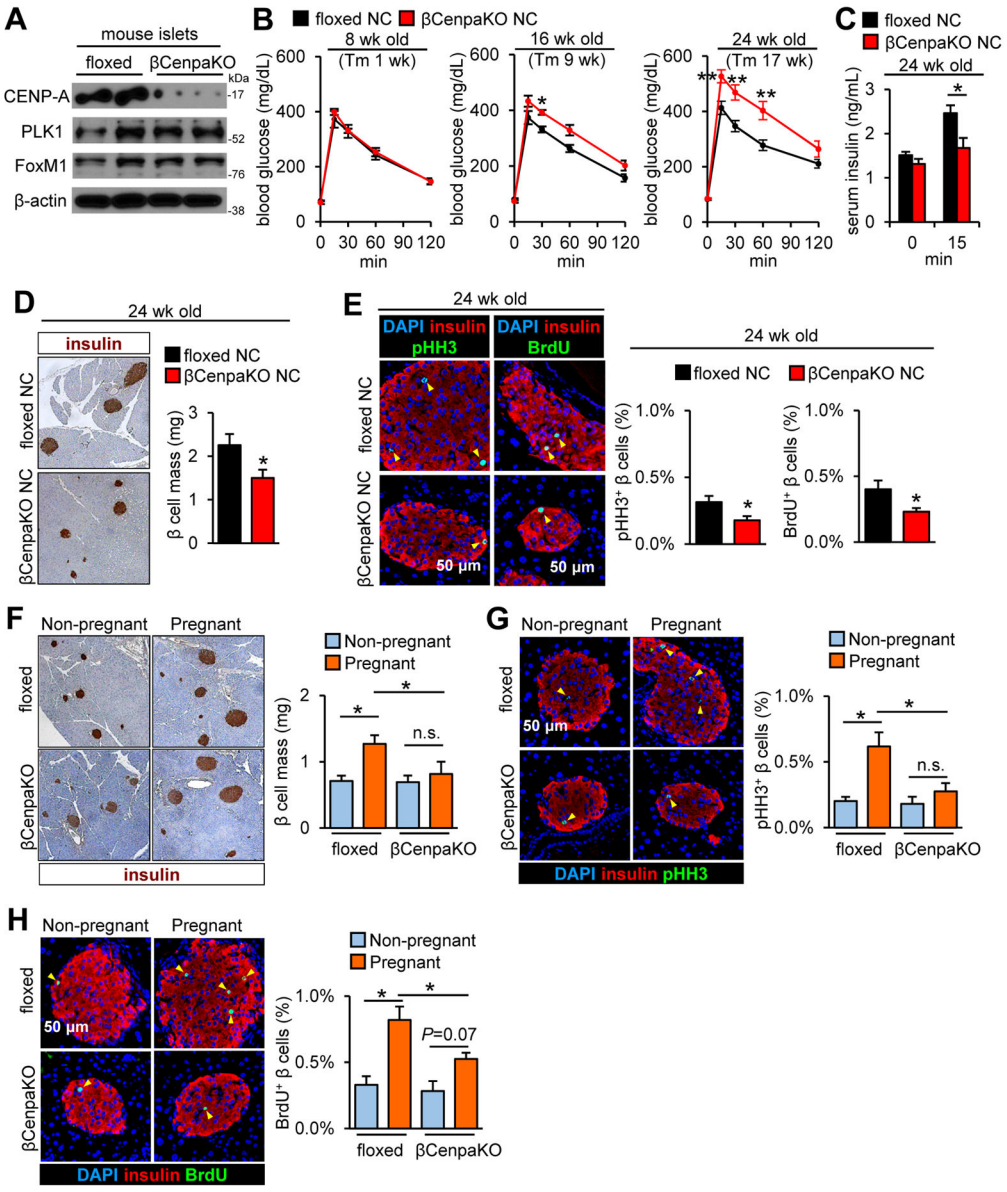

Figure 4. Reduced β-cell proliferation in β-cell-specific CENP-A knockout (βCenpaKO) mouse in response to physiological demands

(A) Western blot of indicated proteins in 12 week-old male floxed and βCenpaKO mouse islets after 4 weeks of tamoxifen injection.

(B and C) Glucose tolerance test. (B) Plasma glucose levels. *p < 0.05, **p < 0.01 (aged 8, 16, or 24 weeks, n=8). (C) Serum insulin levels. *p < 0.05 (aged 24 weeks, n=8).

(D) Left panel; Representative pancreatic sections. Insulin is stained brown. Right panel; β-cell mass. *p < 0.05 (aged 24 weeks, n=5).

(E) Left panel; Representative pancreatic sections. Insulin is stained red, nuclei are stained blue (DAPI), and pHH3+ or BrdU+ or nuclei are stained green. Right panel; Number of pHH3+ or BrdU+ β-cells in the islets. *p < 0.05 (aged 24 weeks, n=5).

(F–H) Virgin mice (Non-pregnant) or mice at gestational day 15.5 of pregnancy (Pregnant).

(F) Left panel; Representative pancreatic sections. Right panel; β-cell mass. *p < 0.05 (n=6).
(G) Left panel; Representative pHH3 staining of endocrine pancreas. Right panel; Number of pHH3+ β-cells in the islets. *p < 0.05 (n=5).
(H) Left panel; Representative BrdU staining of endocrine pancreas. Right panel; Number of BrdU+ β-cells in the islets. *p < 0.05 (n=5).
All data are represented as mean ± SEM in (B–H).
See also Figure S4.

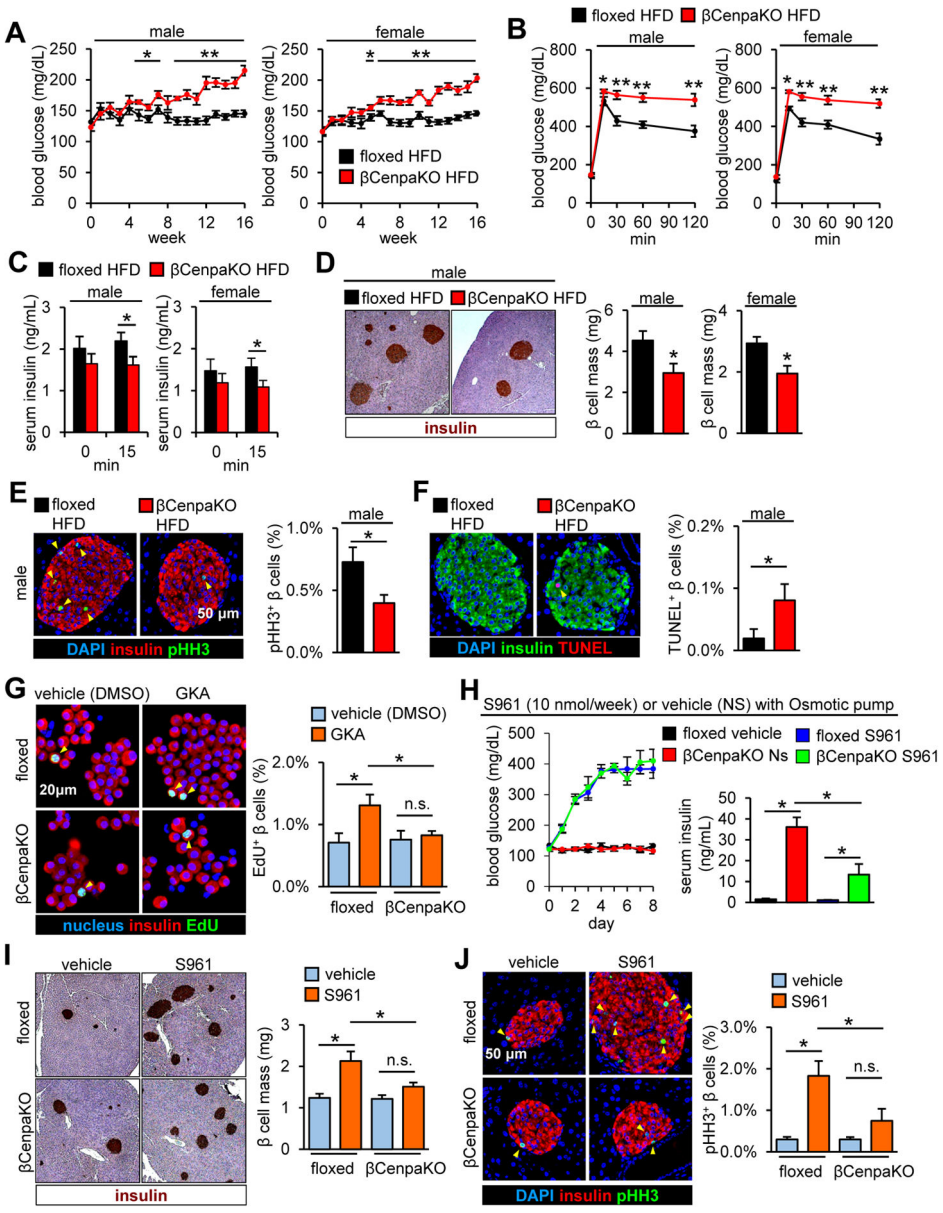

Figure 5. Impaired β-cell proliferation in response to physiological and pathophysiological demands in βCenpaKO mouse

(A) Fed blood glucose levels under high-fat diet (HFD) feeding. *p < 0.05, **p < 0.01 (male, n=7; female, n=15).

(B–F) Experiments were performed on floxed and βCenpaKO mice after 16 weeks on the HFD.

(B and C) Glucose tolerance test. (B) Plasma glucose levels. *p < 0.05, **p < 0.01 (male, n=7; female, n=8). (C) Serum insulin levels. *p < 0.05 (male, n=7; female, n=8).

(D) Left panel; Representative pancreatic sections. Right panel; β-cell mass. *p < 0.05 (male, n=6; female, n=6).

(E) Left panel; Insulin is stained red, nuclei are stained blue, and pHH3+ nuclei are stained green in HFD-fed mice. Right panel; Number of pHH3+ β-cells in the islets of HFD-fed mice. *p < 0.05 (male, n=5).
(F) Left panel; Insulin is stained green, nuclei are stained blue, and TUNEL+ nuclei are stained red. Right panel; Representative pancreatic sections. Number of TUNEL+ β-cells in the islets. *p < 0.05 (male, n=7).
(G) Isolated islets were incubated with 30μM glucokinase activator (GKA) or vehicle for 24 hours at 5.6 mmol/L glucose. Left panel; Representative images of dispersed islet cells. Insulin is stained red, nuclei are stained blue, and EdU+ nuclei are stained green. Right panel; Number of ErdU+ β-cells in the dispersed islets. *p < 0.05 (aged 12 weeks, n=4).
(H–J) Mice were administrated S961 (10 nM/week) or vehicle (Ns) by osmotic pump for 8 days.
(H) Fed blood glucose levels (left) and serum insulin levels at the end of the 8-day infusion period (right). *p < 0.05 (n=5).
(I) Left panel; Representative pancreatic sections. Right panel; β-cell mass. *p < 0.05 (n=5).
(J) Left Panel; Representative pHH3 staining of endocrine pancreas. Right panel; Number of pHH3+ β-cells in the islets of S961- or vehicle-treated mice. *p < 0.05 (n=5).
All data are represented as mean ± SEM in (A–J).
See also Figure S5.

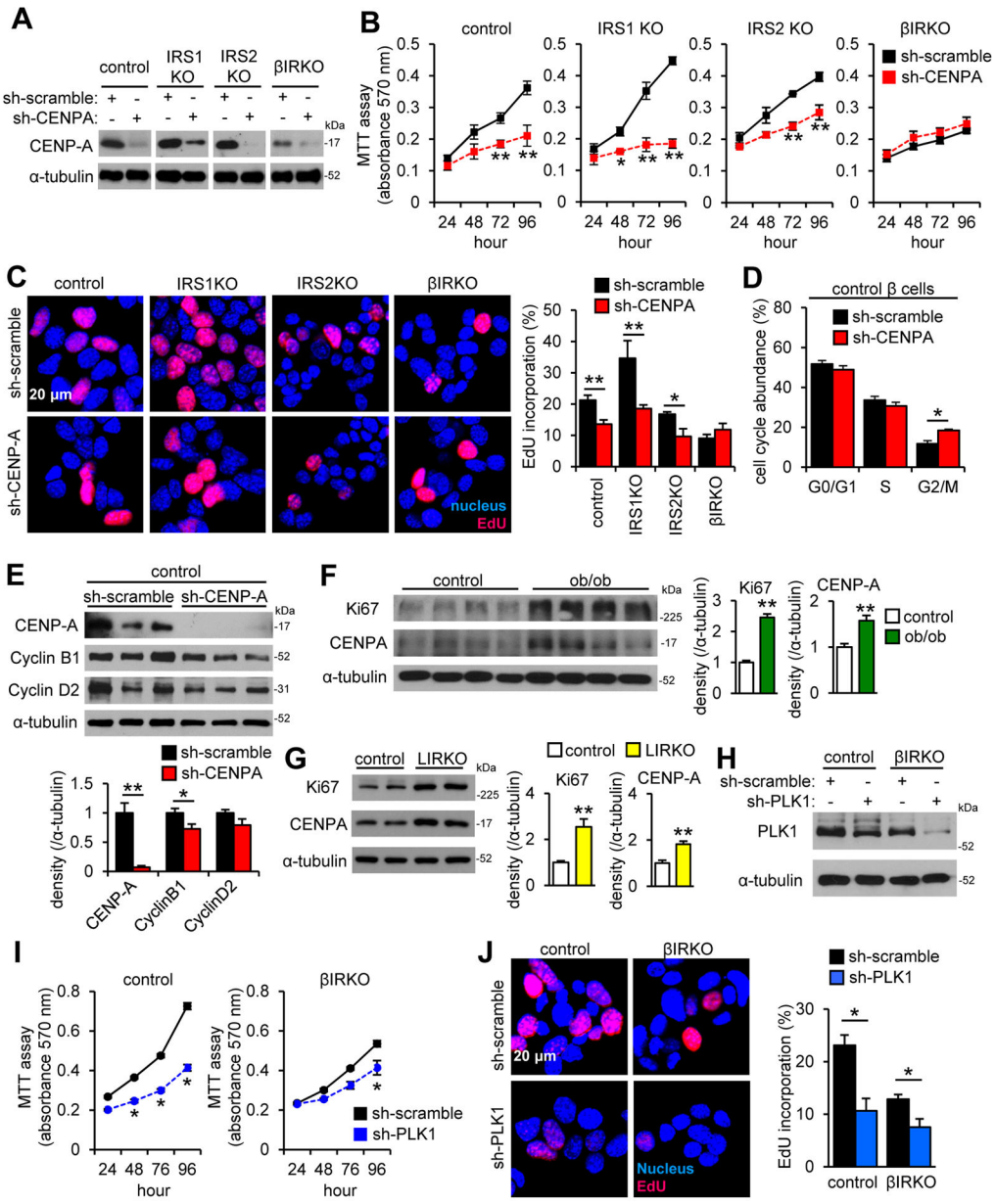

Figure 6. Reduced proliferation in CENP-A and PLK1 knockdown β-cell lines

(A) Western blot of CENP-A and α-tubulin in β-cell lines transduced with lentivirus expressing sh-scramble or sh-CENP-A.

(B) MTT assay in indicated cells. *$p < 0.05$ (n=6).

(C) Left panel; Representative images of β-cell lines. Nuclei are stained blue, and EdU+ nuclei are stained red. Right panel; Number of ErdU+ β-cells. *$p < 0.05$, **$p < 0.01$ (n=4).

(D) Cell cycle distribution of indicated cells. *$p < 0.05$ (n=4).

(E) Upper panel; Western blot of indicated proteins in scramble- or CENP-A-knockdown control β-cells. Lower panel; Intensity of the signals quantified by densitometry. *$p < 0.05$, **$p < 0.01$ (n=5).

(F and G) Left panels; Western blot of indicated proteins in isolated islets from control, ob/ob (F), or LIRKO (G) mice. Right panels; Intensity of the signals quantified by densitometry. **$p < 0.01$ (n=4).

(H) Western blot of PLK-1 and α-tubulin in β-cell lines transduced with lentivirus expressing sh-scramble or sh-PLK1.

(I) MTT cell proliferation assay in indicated cells. *$p < 0.05$ (n=6).

(J) Left panel; Representative images of indicated β-cells. Nuclei are stained blue, and EdU+ nuclei are stained red. Right panel; Number of ErdU+ β-cells. *$p < 0.05$ (n=4).

All data are represented as mean ± SEM in (B–G) and (I–J).

See also Figure S6.

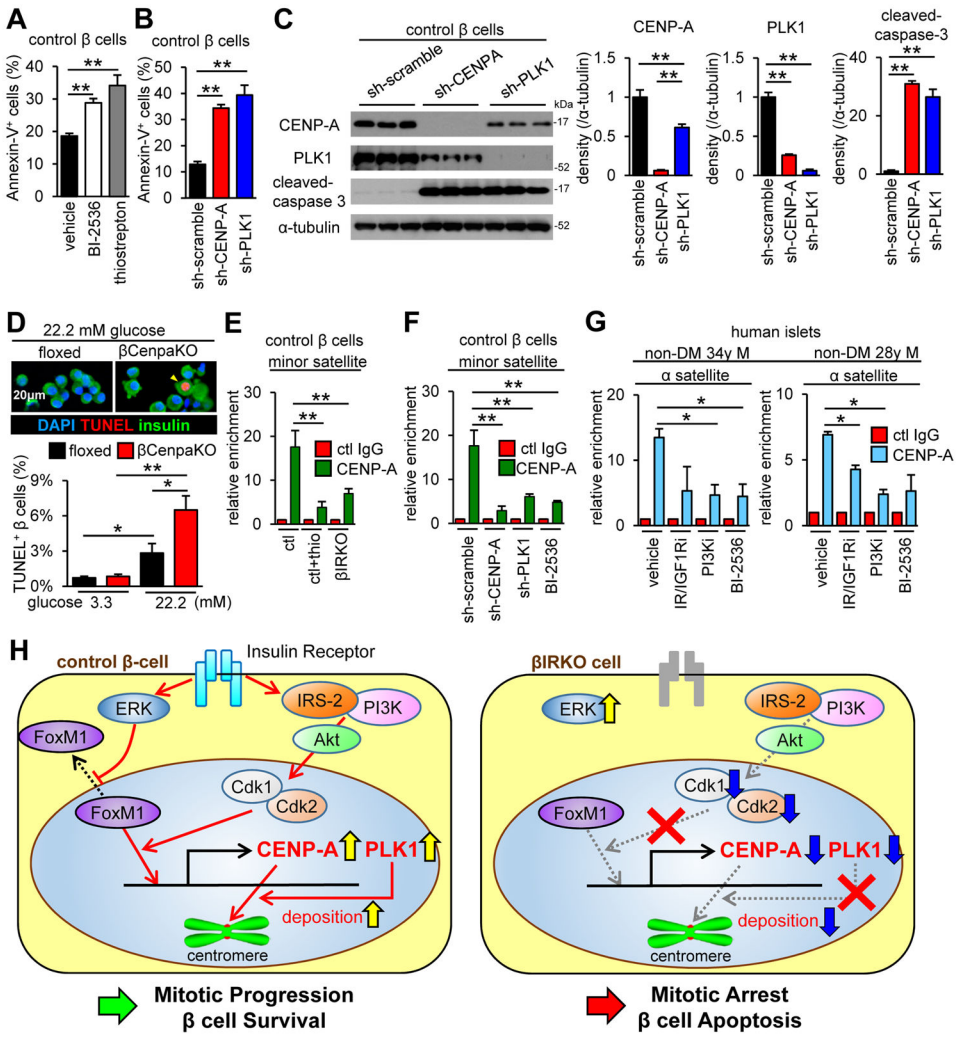

Figure 7. Increased apoptosis in CENP-A knockdown β-cell lines and requirement of PLK for CENP-A deposition

(A) β-cells were treated with BI-2536 or thiostrepton for 24 hours. The proportion of Annexin V+ apoptotic β-cells. **p < 0.01 (n=3).

(B) The proportion of Annexin V+ apoptotic cells of indicated cells. **p < 0.01 (n=3).

(C) Left panel; Western blot of indicated proteins in each knockdown β-cells. Right panel; Intensity of the signals quantified by densitometry. **p < 0.01 (n=6).

(D) Isolated islets were incubated with 3.3 mM or 22.2 mM glucose for 24 hours. Upper panel; Representative images of dispersed islet cells. Insulin is stained green, nuclei are stained blue, and TUNEL+ nuclei are stained red. Lower panel; Number of TUNEL+ β-cells in the dispersed islets. *p < 0.05, **p < 0.01 (aged 9 weeks, n=5).

(E and F) ChIP assays for CENP-A on minor satellite, a mouse centromere marker, in control β-cells in the presence of FoxM1 inhibitor thiostrepton (thio) for 24 hours or in βIRKO β-cells (E, n=4), or in CENP-A- or PLK-1-knockdown control β-cells or in control β-cells in the presence of PLK1 inhibitor BI-2536 (50 nM) for 24 hours (F, n=4). **p < 0.01.

(G) ChIP assays for CENP-A on α satellite, a human centromere marker, in non-DM human islets in the presence of IR/IGF1R dual inhibitor (IR/IGF1Ri), PI3-kinase inhibitor (PI3Ki), or PLK1 inhibitor (BI-2536) for 24 hours. *$p < 0.05$ (n=4).

(H) Schematic of the regulation of CENP-A expression and its deposition to centromere in β-cells.

All data are represented as mean ± SEM in (A–G).

See also Figure S7.